

**Dynamical fermions with fat links**

Francesco Knechtli\* and Anna Hasenfratz†

*Physics Department, University of Colorado, Boulder, Colorado 80309*

(Received 19 December 2000; published 2 May 2001)

We present and test a new method for simulating dynamical fermions with fat links. Our construction is based on the introduction of auxiliary but dynamical gauge fields and works with any fermionic action and can be combined with any fermionic updating. In our simulation we use an overrelaxation step which makes it effective. For four flavors of staggered fermions the first results indicate that flavor symmetry at a lattice spacing  $a \approx 0.2$  fm is restored to a few percent. With the standard action this amount of flavor symmetry restoration is achieved at  $a \approx 0.07$  fm. We estimate that the overall computational cost is reduced by at least a factor of 10.

DOI: 10.1103/PhysRevD.63.114502

PACS number(s): 11.15.Ha, 12.38.Aw, 12.38.Gc

**I. INTRODUCTION**

Improved actions reduce lattice artifacts and thus allow simulations at coarser lattice spacing, larger lattice quark masses and smaller lattice volumes. The use of improved actions in large scale numerical simulations has been increasing steadily. For dynamical simulations a factor of 2 improvement in lattice spacing can easily translate to a gain of 100 in computational cost, which usually more than compensates for the reduction in efficiency of the algorithm. Systematic improvement programs remove lattice artifacts perturbatively [1–4] or nonperturbatively [5–8] by adding irrelevant operators to the action. The use of fat or smeared links is part of many of these improvement programs [9,10]. Smearing the links of a lattice action does not change the long-distance properties of the system, but by smoothing out short scale lattice vacuum fluctuations, it reduces lattice artifacts. Fat link actions by themselves show improved scaling properties, especially in quantities most sensitive to short distance fluctuations.

For Wilson-type clover fermions, chiral properties show significant improvement in fat link quenched simulations [11]. Fattening removes many small dislocations and that reduces the spread of the real eigenmodes of the Dirac operator and the occurrence of exceptional configurations. The perturbation theory for fat-link Wilson-type fermions has been worked out in [12], showing that the additive mass renormalization is small, the renormalization factors are very close to one and the tree-level clover coefficient  $c_{\text{SW}} = 1.0$  is expected to be close to the nonperturbative value.

Fat links have also been successfully used in overlap actions [13,14]. The improved chiral properties of fat link actions result in significantly faster convergence in evaluating Neuberger's formula.

The use of fat links with staggered fermions improves flavor symmetry. In the staggered fermion formulation the four components of a Dirac spinor occupy different lattice sites and connect to different gauge fields, leading to flavor symmetry breaking. The flavor symmetry breaking is espe-

cially evident for the pions: only one of the pseudoscalar mesons is a true Goldstone particle; the others are massive even at vanishing quark mass. Since flavor symmetry breaking is basically due to the fluctuations of the gauge fields within a hypercube and is particularly sensitive to dislocations, local smearing of the gauge links is very effective in reducing flavor symmetry breaking. Several quenched simulations verified this conjecture [15–17]. Dynamical simulations with one level of smearing [18,19] found similar improvement. Perturbative studies of flavor symmetry breaking also support the use of fat links [20].

Dynamical simulation of fermion actions with fat links can be very complicated. Even in the simplest case where the fat link is constructed as a sum of several paths connecting the fermions, the fermionic force term will have many more terms than with thin link action. If the fat link is projected back to SU(3) and the fattening procedure is iterated (as proved to be most effective in quenched simulations), direct calculation of the fermion force term becomes nearly impossible.

In this article we present a new method for simulating fat link fermion actions with many levels of projected smearing. The basic idea is to introduce an *auxiliary but dynamical gauge field* for each smearing level. These gauge fields couple to each other by blocking kernels representing one level of smearing. The last of the auxiliary gauge fields couple directly to the fermions just like ordinary thin links, thus avoiding the complicated gauge force computations. Our construction does not consider the systematic improvement of the action, but it can be combined with any thin link fermionic action. Combining systematic improvements of a thin link action with fat link fermions can lead to further systematic improvement.

To motivate our choice of fat link action in Sec. II we study flavor symmetry breaking with staggered fermions in the quenched approximation. We consider valence actions with different levels of smearing and we compare the results with the standard thin link action. The quenched simulation suggests that with three levels of projected fat links flavor symmetry improves to a level corresponding to a factor of 2.5 change in lattice spacing.

In Sec. III we present our general construction of a fat link fermion action. We suggest combining different updat-

\*Email address: knechtli@pizero.colorado.edu

†Email address: anna@eotvos.colorado.edu

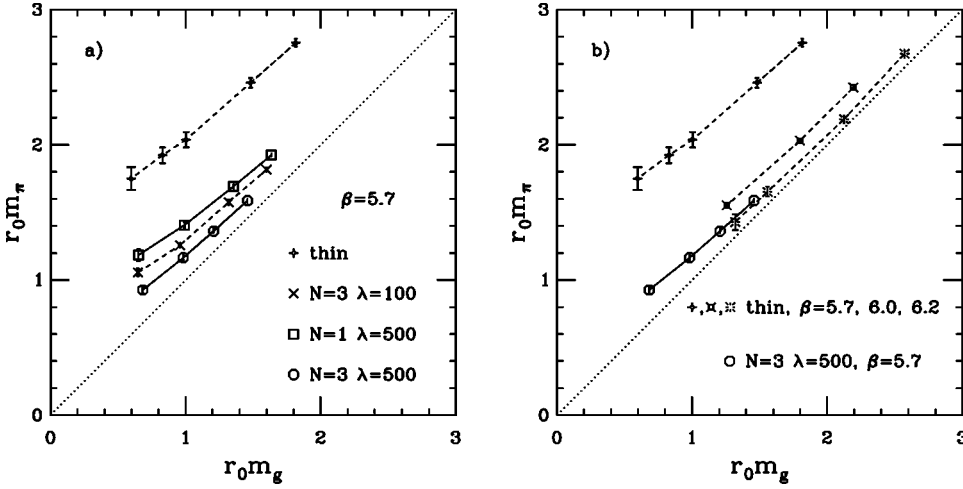


FIG. 1. The mass  $m_\pi$  of the lightest non-Goldstone pion as the function of the mass  $m_g$  of the Goldstone pion in the quenched approximation. (a) shows results for  $\beta=5.7$  using both a thin link and different fat link valence actions. (b) results obtained with our best fat link action on  $\beta=5.7$  background are compared with thin link action results on  $\beta=5.7$ ,  $\beta=6.0$ , and  $\beta=6.2$  background configurations. The lattice spacing changes by a factor of 2.5 between  $\beta=5.7$  and  $\beta=6.2$ .

ing methods in the numerical simulation. The simplest is to update the original and all but the last auxiliary gauge fields using Metropolis updating. The last level auxiliary gauge field couples to the fermions. Any fermionic updating can be used; we consider molecular dynamics updating here.

Unfortunately this coupled system is very rigid and evolves extremely slowly under local updating. In Sec. IV we discuss a global overrelaxation step that improves the situation considerably. Overrelaxation updating based on the gauge action is usually not very effective for fermions [21]. The situation here is quite different. Since the fermions couple to a several times smeared smooth gauge field, we find that one can update up to  $(0.3 \text{ fm})^4$  part of the lattice and still have a large enough acceptance rate to make the algorithm efficient.

In Sec. IV we specify the action for four flavors of staggered fermions and discuss the overrelaxation update in detail. One iteration of our algorithm is composed of 100 overrelaxation, one Metropolis and one molecular dynamics steps. This combined updating is about 15–20 times slower than a molecular dynamics thin link updating and has about the same autocorrelation times. Considering that we gain well over a factor of 100 from the improved scaling properties, this cost is acceptable. Our first results with this algorithm confirm the quenched results for flavor symmetry breaking. We find that flavor symmetry violations are reduced to a few percent at a lattice spacing  $a \approx 0.20 \text{ fm}$ .

In Sec. V we summarize our results and discuss the future directions.

## II. FAT LINK ACTIONS AND QUENCHED SPECTROSCOPY

In this section we investigate the spectrum of fat link staggered actions in the quenched approximation. Previous extensive studies [17] have demonstrated the improvement in the restoration of flavor symmetry due to the smearing of the gauge links. Our goal here is to motivate the parameters of our dynamical fat link action.

We fatten the gauge links using APE smearing [22]: the smeared or fat link  $Q$  is constructed from the thin link  $U$  as

$$Q_{i,\mu} = (1 - \alpha)U_{i,\mu} + \frac{\alpha}{6} \sum_{i,\mu} (U), \quad (1)$$

where  $\sum_{i,\mu} (U)$  is the sum over the six staples around the link  $U_{i,\mu}$ . We use the index  $i$  to label the lattice sites and the index  $\mu$  to label the four space-time directions. The smearing procedure, Eq. (1), can be iterated if the fat link  $Q$  is projected onto  $SU(3)$ :

$$W_{i,\mu} = \text{Proj}_{SU(3)}\{Q_{i,\mu}\}. \quad (2)$$

The  $n$ th level fat link is given by

$$Q_{i,\mu}^{(n)} = (1 - \alpha)W_{i,\mu}^{(n-1)} + \frac{\alpha}{6} \sum_{i,\mu} (W^{(n-1)}), \quad (3)$$

where  $\sum_{i,\mu} (W^{(n-1)})$  is the sum of staples around  $W_{i,\mu}^{(n-1)}$ , the  $(n-1)$ th level fat link projected onto  $SU(3)$  ( $W^{(0)} \equiv U$ ). In the following we label by  $N$  the number of smearing iterations or levels. Perturbative arguments [12] show that for values of the smearing parameter  $0 \leq \alpha \leq 0.75$  the smearing orders the gauge configuration suppressing small scale fluctuations. If  $\alpha > 0.75$ , the smearing eventually disorders. In the following we choose, somewhat arbitrarily,  $\alpha = 0.70$ .

We consider two different  $SU(3)$  projections: a *deterministic* projection  $W_{\max,i,\mu}$  defined by

$$\text{Re Tr}(W_{\max,i,\mu} Q_{i,\mu}^\dagger) = \max_{W \in SU(3)} \text{Re Tr}(W Q_{i,\mu}^\dagger) \quad (4)$$

and a *probabilistic* projection  $W_{i,\mu}^\lambda$ , where  $W_{i,\mu}^\lambda$  is chosen according to the probability distribution

$$P(W) \propto \exp\left[\frac{\lambda}{3} \text{Re Tr}(W Q_{i,\mu}^\dagger)\right] \quad (5)$$

with projection parameter  $\lambda$ . For  $\lambda = \infty$ , Eq. (5) is equivalent to Eq. (4).

To illustrate the effect of fat links on flavor symmetry restoration we calculated the pion spectrum on a set of  $8^3 24$ ,  $\beta=5.7$  ( $a=0.17 \text{ fm}$ ) quenched lattices. In Fig. 1(a) we plot the masses of the (would-be) Goldstone pion  $\pi_g$  and the lightest non-Goldstone pion,  $\pi_{15}$ , corresponding to the representation  $\gamma_5 \otimes \gamma_i \gamma_5$ . We label the representation of the states following [23,24] by  $\Gamma_S \otimes \Gamma_F$ , where  $\Gamma_S$  labels the

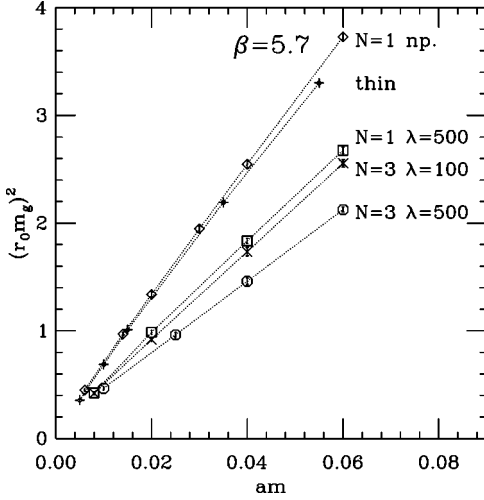


FIG. 2. The mass renormalization in the quenched approximation at  $\beta=5.7$  for the thin link and different fat link valence actions. In addition to the actions used in Fig. 1, we show the results for  $N=1$  level of nonprojected (np.) APE smearing.

spin and  $\Gamma_F$  labels the  $SU(4)$  flavor. The pion masses are expressed in units of the Sommer scale  $r_0$  ( $r_0=2.87a$  at  $\beta=5.7$ ) [25]. In addition to the thin link we consider three fat link valence actions:  $N=1$  and  $N=3$  levels of smearing with projection parameter  $\lambda=500$  and  $N=3$  levels of smearing with projection parameter  $\lambda=100$ , all with  $\alpha=0.7$ . We observe considerable improvement from  $N=1$  to  $N=3$ . Also,  $\lambda=100$  for the projection parameter is clearly not as effective as  $\lambda=500$ . Increasing the number of blocking levels,  $N$ , or the projection parameter  $\lambda$  further does not improve the situation substantially but increases the computational effort considerably. In the rest of this paper we will consider the fat link action corresponding to  $N=3$  levels of blocking with projection parameter  $\lambda=500$  and APE parameter  $\alpha=0.7$ . While these parameters are not unique, they seem to be close to optimal.

To get a feel for the amount of improvement one can achieve with this fat link action, in Fig. 1(b) we compare the  $N=3$ ,  $\lambda=500$  action with thin link data at  $\beta=5.7$ , 6.0, and 6.2. The data for the last two  $\beta$  values are from Ref. [24] and correspond to lattice spacings  $a=0.095$  fm and 0.069 fm and Sommer parameters  $r_0=5.26a$  and  $7.25a$ , respectively [26]. The  $N=3$ ,  $\lambda=500$  smearing reduces flavor symmetry violations on the  $\beta=5.7$  configurations to the level obtained at  $\beta=6.2$  with thin link action, a factor of 2.5 improvement in lattice spacing. The computational cost of full QCD grows at least as  $1/a^6$  [3] and for certain quantities even as  $1/a^{10}$  [27]. A factor of 2.5 in the lattice spacing means a factor of  $200-10^4$  in computational cost.

Finally, in Fig. 2 we plot the square of the Goldstone-pion mass as a function of the bare quark mass. All measurements are on the  $\beta=5.7$  gauge configurations using thin link and different fat link actions. In addition to the actions considered in Fig. 1, we show the results for  $N=1$  level of nonprojected APE smearing. Fat link perturbation theory predicts that the mass renormalization constant becomes perturbative as  $N$  increases. We see that the mass renormal-

ization after one level of nonprojected smearing is almost the same as without smearing. Increasing the smearing level and the value of  $\lambda$  indeed reduces the multiplicative mass renormalization factor.

### III. DYNAMICAL FERMIONS WITH FAT LINKS

The quenched results show that smearing the gauge links considerably improves the flavor symmetry of staggered fermions. There is evidence that these results carry over to dynamical simulations [18] where one level of smearing is implemented. Because of the gauge force computations in the molecular dynamics equations of motion, it is very complicated to simulate fermions with many levels of smearing, even impossible if projection of the gauge links into  $SU(3)$  is made after each smearing step.

Our method to overcome this difficulty is to introduce a set of *auxiliary but dynamical gauge fields* which couple to each other in the action by blocking kernels representing one level of smearing. The last level auxiliary gauge field couples directly to the fermions in the same way the usual thin links do. The problem of the computations of the gauge force is transferred to the gauge sector where it can be solved. This construction can be used for any fermion action which can be simulated with thin links.

Let us start considering fermions coupled to fat links constructed with one level of smearing from the thin links  $U_{i,\mu}$ . We introduce a dynamical auxiliary gauge field  $V$  and we define the action

$$S = -\frac{\beta}{3} \sum_p \text{Re Tr}(U_p) - \frac{\lambda}{3} \sum_{i,\mu} \text{Re Tr}[V_{i,\mu} W_{\text{max},i,\mu}^\dagger(U)] - \text{tr} \ln[M^\dagger(V)M(V)]. \quad (6)$$

Here  $p$  labels the plaquettes  $U_p$ ,  $W_{\text{max}}(U)$  is the  $SU(3)$  projection, Eq. (4), of the fat link given in Eq. (1) and  $M(V)$  is the fermion matrix. The blocking parameter  $\lambda$  constrains the auxiliary gauge links  $V_{i,\mu}$  to be close to the projected fat links  $W_{\text{max},i,\mu}(U)$ . Fluctuations of the field  $V$  are proportional to  $1/\lambda$ . This is a dynamical realization of the projection Eq. (5). In Eq. (6),  $\text{Tr}$  means the trace over  $SU(3)$  color whereas  $\text{tr}$  means the overall trace over space-time indices  $i$ , directions  $\mu$ , spin and color.

For many levels of smearing, we introduce a set of dynamical auxiliary gauge fields  $W^{(1)}, W^{(2)}, \dots, W^{(N)} \equiv V$ , one for each level of smearing. The action, Eq. (6), is generalized to

$$S = -\frac{\beta}{3} \sum_p \text{Re Tr}(U_p) - \frac{\lambda}{3} \sum_{i,\mu} \text{Re Tr}[W_{i,\mu}^{(1)} W_{\text{max},i,\mu}^\dagger(U)] - \frac{\lambda}{3} \sum_{i,\mu} \text{Re Tr}[W_{i,\mu}^{(2)} W_{\text{max},i,\mu}^\dagger(W^{(1)})] \cdots - \frac{\lambda}{3} \sum_{i,\mu} \text{Re Tr}[V_{i,\mu} W_{\text{max},i,\mu}^\dagger(W^{(N-1)})] - \text{tr} \ln[M^\dagger(V)M(V)]. \quad (7)$$

This action is in the same universality class as the original thin link action. If the blocking parameter is  $\lambda = \infty$ , the auxiliary gauge fields can be integrated out and the resulting action is a plaquette gauge action while the fermions couple to deterministically projected fat links. If  $\lambda \neq \infty$ , the integration of the auxiliary gauge fields will introduce additional gauge terms. These new terms depend on the thin link variables in a complicated way, but they are all local terms containing only a finite number of link variables. Thus, these terms do not change the universality class of the action.

The updating of this system can, in principle, be done by a sequence of Metropolis updates for the fields  $U, W^{(1)}, \dots, W^{(N-1)}$  and by the standard updating for the fermion matrix  $M$ , with the only difference that now the last auxiliary gauge field  $V$  enters the fermion matrix.

The problem of this basic algorithm is that the system with large  $\lambda$  is very rigid and evolves very slowly. To cure this problem, we use a hybrid overrelaxation algorithm [28–37] with (i) Metropolis updating for the gauge fields  $U, W^{(1)}, \dots, W^{(N-1)}$ , (ii) standard algorithm for the fermion matrix  $M(V)$  and (iii) *global overrelaxation* for all the gauge fields  $U, W^{(1)}, \dots, V$ .

In the next section we discuss how an overrelaxation can be implemented. It plays a key role in reducing the autocorrelation times of the Metropolis update. Note that the overrelaxation update is effective only because the fermions couple to the smooth fat links.

#### IV. OVERRELAXATION WITH FAT LINKS

Our overrelaxation update is based on the usual overrelaxation reflection step used in pure gauge systems that leaves the gauge action invariant [32,33]. We reflect the thin links just like in the standard overrelaxation algorithm by sweeping in a given order through some part (or all) of the lattice:

$$U \rightarrow U'. \quad (8)$$

These changes are followed by a transformation of the fat links:

$$W^{(1)'} = W^{(1)} W_{\max}^\dagger(U) W_{\max}(U'), \quad (9)$$

$$W^{(2)'} = W^{(2)} W_{\max}^\dagger(W^{(1)}) W_{\max}(W^{(1)'}), \quad (10)$$

...

$$V' = V W_{\max}^\dagger(W^{(N-1)}) W_{\max}(W^{(N-1)'}). \quad (11)$$

All links for a given level are reflected and then the next level gauge field is changed. The reflections must be performed in the order given by Eqs. (8)–(11). This transformation leaves the gauge part of the action invariant, but the fermionic part will change and a Metropolis accept-reject step must be performed. In order for this updating to satisfy detailed balance, the probability  $P$  for changing the gauge field configuration  $\{U, W^{(1)}, \dots, V\}$  to  $\{U', W^{(1)'}, \dots, V'\}$  has to be equal to the probability for the reversed change: i.e.,

$$\begin{aligned} P(\{U, W^{(1)}, \dots, V\} \rightarrow \{U', W^{(1)'}, \dots, V'\}) \\ = P(\{U', W^{(1)'}, \dots, V'\} \rightarrow \{U, W^{(1)}, \dots, V\}). \end{aligned} \quad (12)$$

This can be achieved by choosing with probability 1/2 either a given sequence of the thin link reflections, Eq. (8), or with equal probability the reversed sequence [21]. The sequence has to be reversed with respect to the direction and location of the thin links and with respect to the index of the SU(2) subgroup. The thin link reflections are then followed by the local reflections, Eqs. (9)–(11), for the auxiliary gauge links. For a given level of auxiliary gauge field the reflections are independent of the order with which we sweep through the lattice and they are symmetric under exchange of primed and unprimed quantities. If we start from a gauge field configuration  $\{U, W^{(1)}, \dots, V\}$  and apply Eqs. (8)–(11) twice with the sequence of thin link reflections reversed, we come back to the original configuration. This overrelaxation algorithm satisfies detailed balance and is a legal update of the system. To achieve ergodicity though, one must still perform some updates with the basic algorithm.

For the Metropolis accept-reject step following the changes, Eqs. (8)–(11), we have to calculate the action; i.e., we need an explicit form of the determinant to evaluate. For four flavors of staggered and two flavors of Wilson fermions this is trivially realized. In terms of pseudofermion fields  $\Phi$  the action, Eq. (7), is

$$S = S_g(U, W^{(1)}, \dots, V) + \Phi^\dagger [M^\dagger(V)M(V)]^{-1} \Phi, \quad (13)$$

where  $M(V)$  represents the fermion matrix. The equilibrium probability distribution of the gauge fields  $U, W^{(1)}, \dots, V$  is given by

$$P_{\text{eq}}(U, W^{(1)}, \dots, V) \propto e^{-S_g(U, W^{(1)}, \dots, V)} \det[M^\dagger(V)M(V)]. \quad (14)$$

Since the pure gauge part of the action is invariant under the overrelaxation move of the system, the acceptance probability is

$$P_{\text{acc}}(V', V) = \min \left\{ 1, \frac{\det[M^\dagger(V')M(V')]}{\det[M^\dagger(V)M(V)]} \right\}. \quad (15)$$

$P_{\text{acc}}$  depends only on the last level auxiliary gauge links. The goal is to efficiently compute the acceptance probability.

Instead of calculating the determinant in Eq. (14) we use a stochastic estimator to approximate  $P_{\text{acc}}$  [38,39]:

$$P'_{\text{acc}}(V', V) = \min \{ 1, e^{\xi^\dagger [M^\dagger(V')M(V') - M^\dagger(V)M(V)] \xi} \}, \quad (16)$$

where the vector  $\xi$  is generated according to the distribution

$$P(\xi) \propto e^{-\xi^\dagger M^\dagger(V')M(V') \xi}. \quad (17)$$

After configuration averaging, this procedure satisfies the detailed balance condition [39].

If the gauge fields  $V$  and  $V'$  are very different, the acceptance rate from Eq. (16) will be small even when the fermionic determinants are actually very close. This is because of the large fluctuations of the stochastic estimator. To improve the acceptance rate, we attempt to remove the most ultraviolet part of the fermionic matrix and include it explicitly as an effective gauge action. The resulting reduced matrix gives a much higher acceptance in Eq. (16).

For heavy fermions the fermion determinant gives rise to an effective plaquette term for the gauge field [40]. Even for small quark masses the ultraviolet part of the fermion determinant can be well approximated by an effective loop action involving only small Wilson loops [41–43]. These observations suggest to remove the plaquette term from the fermion matrix by introducing a reduced matrix  $M_r$  as

$$M(V) = M_r(V)A(V) \quad \text{with} \quad (18)$$

$$A(V) = e^{\alpha_4 D^4(V) + \alpha_2 D^2(V)}, \quad (19)$$

where  $D$  is the kinetic part of the fermion matrix. In terms of  $M_r$  the fermion determinant becomes

$$\det[M^\dagger(V)M(V)] = \det[M_r^\dagger(V)M_r(V)]e^{-S_{\text{eff}}(V)}, \quad (20)$$

---


$$P''_{\text{acc}}(V', V) = \min\{1, e^{S_{\text{eff}}(V) - S_{\text{eff}}(V') + \xi^\dagger [M_r^\dagger(V')M_r(V') - M_r^\dagger(V)M_r(V)]\xi}\}. \quad (24)$$

In practice, we start by generating a random Gaussian source  $R$  according to the probability distribution

$$P(R) \propto e^{-R^\dagger R} \quad (25)$$

from which we form the vectors

$$\Phi' = M^\dagger(V')R, \quad (26)$$

$$X' = [M^\dagger(V')M(V')]^{-1}\Phi'. \quad (27)$$

The vector  $\xi$  in Eq. (23) is then given by  $\xi = A(V')X'$  and we can write the fermionic terms in Eq. (24) as

$$\xi^\dagger M_r^\dagger(V')M_r(V')\xi = \Phi'^\dagger X', \quad (28)$$

$$\begin{aligned} \xi^\dagger M_r^\dagger(V)M_r(V)\xi &= X'^\dagger A^\dagger(V')A^\dagger(V)^{-1}M^\dagger(V)M(V) \\ &\quad \times A(V)^{-1}A(V')X'. \end{aligned} \quad (29)$$

The acceptance probability strongly depends on the parameters  $\alpha_2$  and  $\alpha_4$ . The optimal value can be found numerically. We will discuss our choice in the next section.

This procedure is not effective if the fermion matrix depends on thin links, because the fluctuations in the stochastic estimator are too large even after the removal of the  $D^4$  and

$$\begin{aligned} S_{\text{eff}}(V) &= -2\alpha_4 \text{Re tr}[D^4(V)] \\ &\quad - 2\alpha_2 \text{Re tr}[D^2(V)]. \end{aligned} \quad (21)$$

The effective action  $S_{\text{eff}}(V)$  can be evaluated explicitly. In general it is the sum of a plaquette term coming from  $\text{tr}[D^4(V)]$  and a constant from  $\text{tr}[D^2(V)]$ . The real parameters  $\alpha_2$  and  $\alpha_4$  are free and can be optimized. In a different context, a decomposition of the fermion matrix like Eq. (18) has been proposed in [21] motivated by the hopping parameter expansion.

In terms of  $S_{\text{eff}}(V)$  and  $M_r(V)$  the acceptance probability is

$$P_{\text{acc}}(V', V) = \min\left\{1, \frac{e^{-S_{\text{eff}}(V')} \det[M_r^\dagger(V')M_r(V')]}{e^{-S_{\text{eff}}(V)} \det[M_r^\dagger(V)M_r(V)]}\right\}. \quad (22)$$

It can be approximated by generating a vector  $\xi$  according to the distribution

$$P(\xi) \propto e^{-\xi^\dagger M_r^\dagger(V')M_r(V')\xi} \quad (23)$$

and Eq. (22) becomes

---

$D^2$  terms. When the links in the fermion matrix are smeared, these fluctuations are constrained. This is the key feature which makes the overrelaxation effective with fat links.

## V. PERFORMANCE OF THE ALGORITHM

For testing our fat link action we decided to simulate  $N_f = 4$  flavors of staggered fermions. The fermion matrix is given by

$$M(V)_{i,j} = 2m \delta_{i,j} + \sum_{\mu} \eta_{i,\mu} (V_{i,\mu} \delta_{i,j-\hat{\mu}} - V_{i-\hat{\mu},\mu}^\dagger \delta_{i,j+\hat{\mu}}), \quad (30)$$

where  $\eta_{i,\mu}$  are the staggered phases. We impose antiperiodic boundary conditions in the time direction. The pseudofermion field  $\Phi$  and the matrix  $M^\dagger(V)M(V)$  are restricted to the even sites of the lattice [44]. The matrix  $D$  used in Eq. (19) is given by

$$D_{i,j} = \sum_{\mu} \eta_{i,\mu} (V_{i,\mu} \delta_{i,j-\hat{\mu}} - V_{i-\hat{\mu},\mu}^\dagger \delta_{i,j+\hat{\mu}}). \quad (31)$$

The traces in  $S_{\text{eff}}(V)$  in Eq. (21) are computed by summing over the even sites only and give

$$\begin{aligned} \text{tr}[D^4(V)] = & 24\Omega \left[ 3 - \frac{1}{6\Omega} \sum_p \text{Re Tr}(V_p) \right] + 108\Omega \\ & - 4 \delta_{N_t,4} \sum_{i,t=0} \text{Re Tr}(P_i), \end{aligned} \quad (32)$$

$$\text{tr}[D^2(V)] = -12\Omega. \quad (33)$$

$\Omega$  denotes the total number of lattice points and we assume that there are more than 4 sites in each spacelike direction. For  $N_t=4$  sites in the timelike direction there is an extra contribution to  $\text{tr}[D^4(V)]$  coming from the Polyakov lines  $P_i$  starting at location  $i, t=0$ . The minus sign of the Polyakov line in Eq. (32) is due to the antiperiodic boundary conditions in time direction.

As we described in Sec. II we choose the number of auxiliary gauge fields and the smearing parameters to be

$$N=3, \quad \alpha=0.7, \quad \lambda=500. \quad (34)$$

The global overrelaxation (GOR) described in Sec. IV is essential here as it considerably reduces the autocorrelations of the otherwise very rigid system. The GOR leaves the pure gauge action of our system invariant but is subjected to an accept-reject step which accounts for the ratio of fermion determinants, see Eq. (24). Since the fermions couple directly to the last level dynamical fat links, the acceptance rate  $\alpha_{\text{GOR}}$  is large enough to make the algorithm effective.

The parameters  $\alpha_2$  and  $\alpha_4$  entering Eq. (19) are chosen to maximize the acceptance rate  $\alpha_{\text{GOR}}$ . We use

$$\alpha_2 = -0.18, \quad \alpha_4 = -0.006. \quad (35)$$

Setting  $\alpha_2 = \alpha_4 = 0$ , i.e., computing the ratio of fermion determinants without decomposing the fermion matrix according to Eqs. (18) and (19), gives a value for  $\alpha_{\text{GOR}}$  which is a factor of 10 smaller than what we achieve with our choice. Moreover, keeping  $\alpha_4 = 0$  and varying only  $\alpha_2$  gives significantly lower  $\alpha_{\text{GOR}}$ . The choice of Eq. (35) is not unique; we identified in the  $\alpha_2$ - $\alpha_4$  parameter space a bandlike region in which  $\alpha_{\text{GOR}}$  reaches its maximal value.

Even with our improved GOR it is not possible to change simultaneously all the  $U$  links; the effectiveness of the algorithm would be very low. Instead we choose a random block of  $U$  links containing  $(N_{\text{GOR}}/4)$  sites and reflect only the links within this block. These changes propagate more and more through the lattice as we consider the cascade of reflections Eqs. (8)–(11), as 19 fat links have to be changed by changing one link. In Fig. 3 we plot the volume of the lattice in which the  $U$  links are effectively updated (actually the fourth root of it), i.e.,  $(\alpha_{\text{GOR}} N_{\text{GOR}}/4)^{1/4} a$  as a function of the physical volume of the ‘‘touched’’  $U$  links  $(N_{\text{GOR}}/4)^{1/4} a$ . These results are obtained on  $8^3 24$ ,  $\beta=5.2$  and  $am=0.1$  lattices. The lattice spacing from the string tension can be estimated as  $a \approx 0.2$  fm and the correlation length as  $r_0 m_g \approx 1.7$ . We see in Fig. 3 that there is a maximal physical volume

$$V_{\text{GOR}} \approx (0.3 \text{ fm})^4 \quad (36)$$

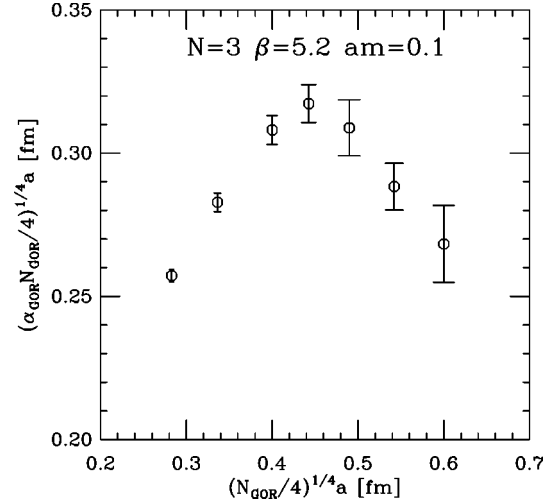


FIG. 3. The effective physical volume where the  $U$  links change in one global overrelaxation (GOR) updating step as function of the physical volume ‘‘touched.’’ The results are obtained on  $8^3 24$  lattices.

which can be updated with a reasonable acceptance rate. The actual value of  $\alpha_{\text{GOR}}$  depends on the number of ‘‘touched’’ links  $N_{\text{GOR}}$ . The broad maximum in Fig. 3 corresponds to  $\alpha_{\text{GOR}}=35\%$  ( $N_{\text{GOR}}=64$ ),  $\alpha_{\text{GOR}}=26\%$  ( $N_{\text{GOR}}=96$ ) and  $\alpha_{\text{GOR}}=16\%$  ( $N_{\text{GOR}}=144$ ) on the above lattices.

We observed that the value, Eq. (36), scales with the lattice spacing. On lattices with smaller lattice spacing more links can be updated at the same time; i.e., the physical volume of the updated region remains fixed. On larger physical volumes, on the other hand, one would have to increase the number of GOR steps to achieve the same efficiency. In our finite-temperature runs on  $8^3 4$  lattices [45] we observed that the effectiveness of the algorithm increases in the deconfined phase. Somewhat surprisingly, the effectiveness also increases with decreasing quark mass. This fact together with the faster convergence of the conjugate gradient (see Table I) allows simulations at quark masses that are not practically possible with the standard thin link action.

In simulating the  $8^3 24 \approx 20 \text{ fm}^4$  lattices, we found it effective to follow each Metropolis and hybrid Monte Carlo (HMC) algorithm by 100 GOR updating steps, each reflecting about a  $(0.3 \text{ fm})^4$  section of the thin link lattices. For timing our algorithm we consider the computer time necessary for 100 GOR steps, one Metropolis (MET) step for each gauge field  $U, W^{(1)}, W^{(2)}$  and one HMC trajectory for the  $V$  field with step size  $\Delta t=0.015$  and  $N_{\text{traj}}=30$  steps. We compare this to the time of one HMC trajectory with step size  $\Delta t=0.015$  and  $N_{\text{traj}}=30$  steps for the thin link action [46,47] with parameters  $\beta=5.25$  and  $am=0.06$ . With these parameters the lattice spacings and the physical quark masses of the two actions are approximately matched. To compare the times for one updating iteration is fair because the autocorrelations for simple observables like the plaquette or the chiral condensate  $\bar{\psi}\psi$  are observed to be the same for the two algorithms in these time units.

In Table I we show the results of the timing comparison. We use one iteration of ordinary thin link HMC algorithm as

TABLE I. Timings for simulation of ordinary thin link HMC algorithm compared to simulation of our algorithm with  $N=3$  auxiliary gauge fields. The dynamical lattices are  $8^{324}$  and the lattice spacings and physical quark masses of the two simulations are approximately matched. The time unit is one updating step (consisting of one HMC trajectory) of the ordinary thin link algorithm. The last two columns give the total time costs and the average number of conjugate gradient (CG) iterations needed per inversion of  $M^\dagger M$ .

links	100 GOR	1 MET	1 HMC	total	CG iterations
thin	-	-	1	1	133
fat	11.0	3.5	0.5	15.0	61

time unit. One iteration of our algorithm costs a factor of 15 more but, as pointed out in Sec. II, we can effectively gain a factor of  $10^2$ – $10^4$  in computer time due to improved scaling. With fat links, there is also a considerable reduction (a factor of 2) in the number of conjugate gradient (CG) iterations needed for the inversion of  $M^\dagger M$ , as shown in the last column of Table I.

Finally we consider flavor symmetry restoration on the dynamical fat link lattices. Figure 4 shows the first results obtained with our fat link action on  $8^{324}$  lattices with parameters  $\beta=5.2$ ,  $am=0.1$  (square). The lattice spacing is  $a \approx 0.2$  fm and the Goldstone pion to rho mass ratio is  $m_g/m_\rho=0.71(1)$ , indicating a correlation length  $r_0m_g \approx 1.7$ . This point agrees very well with the quenched results (octagons) taken from Fig. 1: i.e., flavor symmetry violation is reduced to a few percent. To show the improvement due to the smearing of the gauge links, we also ran the standard thin link staggered action with two sets of parameters,  $\beta=5.25$ ,  $am=0.06$  (fancy square) and  $\beta=5.2$ ,  $am=0.06$  (burst). The

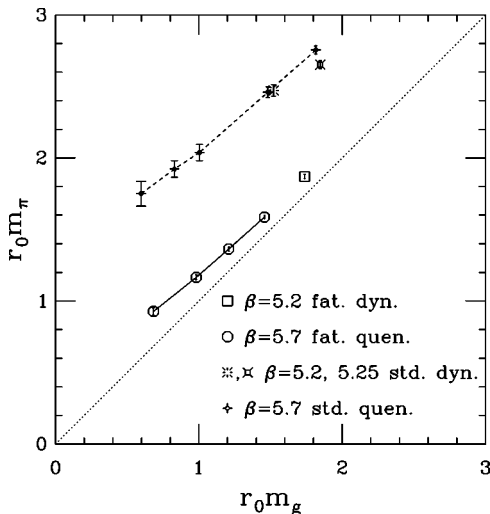


FIG. 4. Flavor symmetry violation for the dynamical runs with our fat link action (fat. dyn.) and with the standard thin link staggered action (std. dyn.). The mass  $m_\pi$  of the lightest non-Goldstone pion is plotted as a function of the mass  $m_g$  of the Goldstone pion (in units of  $r_0$ ). The lattice spacings and the correlation lengths  $r_0m_g$  are approximately matched. For comparison we plot the quenched results from Fig. 1 obtained with the corresponding valence actions (fat. quen. and std. quen.).

lattice spacings from the string tension are approximately  $a \approx 0.18$  fm and  $a \approx 0.22$  fm, and the correlation lengths are  $r_0m_g \approx 1.8$  and  $r_0m_g \approx 1.5$ , respectively. The flavor symmetry violations on the thin link dynamical lattices agree with the quenched predictions (fancy diamonds). Our fat link dynamical action has only about 6% flavor symmetry violation compared to 60% of thin link actions at comparable lattice spacings.

## VI. CONCLUSIONS

We presented a new method for simulating dynamical fermions with fat links constructed through many levels of projected smearing. For each level of smearing we introduce an auxiliary but dynamical gauge field and these gauge fields are connected to each other by blocking kernels representing one level of smearing. Since the last of the auxiliary fields couple in the standard way to the fermions, our construction can be used with any known fermionic update. We discussed the simulation of our system which includes an overrelaxation updating. The fat links entering the fermion matrix make the overrelaxation effective and this is the key feature of our algorithm.

At this time our algorithm is running on scalar machines and the overrelaxation step is worked out for four flavors of staggered fermions. The results for flavor symmetry restoration confirm the quenched results; that is, a factor of 2.5 in the lattice spacing can be gained. Taking into account that our algorithm is about 15–20 times slower than the standard one, this gives an overall gain of at least a factor of 10 in computational costs.

We have used this algorithm to study the finite temperature phase transition of four flavors of staggered fermions at  $N_f=4$  [45]. We observe a qualitative difference compared to thin link simulations. The strongly first order phase transition is washed away; we observe a very broad crossover instead. We believe this difference is due to the improved flavor symmetry. In our simulations we have 15 relatively light pions compared to the single Goldstone particle of thin link simulations.

We are parallelizing the code for large scale simulations [48]. This requires a 32-checkerboard structure but it is not more complicated than parallelizing a Symanzik improved gauge action. The overrelaxation generalizes easily for two flavors of Wilson fermions. To generalize it for two flavors of staggered fermions we need an explicit realization of the action. That can be done by approximating the square root of the fermionic determinant with a polynomial form [49,50]. Our preliminary study shows that it can be done efficiently.

## ACKNOWLEDGMENTS

We are indebted to the MILC Collaboration for the use of their code for standard staggered fermions. We thank Thomas DeGrand for many useful discussions and M. Hasenbusch, F. Niedermayer, and U. Wolff for their important suggestions. This work was supported by the U.S. Department of Energy.

- [1] K. Symanzik, Nucl. Phys. **B226**, 187 (1983).
- [2] K. Symanzik, Nucl. Phys. **B226**, 205 (1983).
- [3] G. P. Lepage, Nucl. Phys. B (Proc. Suppl.) **47**, 3 (1996).
- [4] M. Alford, T. R. Klassen, and G. P. Lepage, Phys. Rev. D **58**, 034503 (1998).
- [5] P. Hasenfratz and F. Niedermayer, Nucl. Phys. **B414**, 785 (1994).
- [6] T. DeGrand, A. Hasenfratz, P. Hasenfratz, and F. Niedermayer, Nucl. Phys. **B454**, 587 (1995).
- [7] T. DeGrand, A. Hasenfratz, P. Hasenfratz, and F. Niedermayer, Nucl. Phys. **B454**, 615 (1995).
- [8] W. Bietenholz and U. J. Wiese, Nucl. Phys. **B464**, 319 (1996).
- [9] MILC Collaboration, T. DeGrand, Phys. Rev. D **58**, 094503 (1998).
- [10] F. Niedermayer, P. Rufenacht, and U. Wenger, Nucl. Phys. **B597**, 413 (2000).
- [11] T. DeGrand, A. Hasenfratz, and T. Kovacs, Nucl. Phys. **B547**, 259 (1999).
- [12] C. Bernard and T. DeGrand, Nucl. Phys. B (Proc. Suppl.) **83**, 845 (2000).
- [13] W. Bietenholz, hep-lat/0007017.
- [14] MILC Collaboration, T. DeGrand, hep-lat/0007046.
- [15] T. Blum *et al.*, Phys. Rev. D **55**, 1133 (1997).
- [16] J. F. Lagae and D. K. Sinclair, Phys. Rev. D **59**, 014511 (1999).
- [17] MILC Collaboration, K. Orginos, D. Toussaint, and R. L. Sugar, Phys. Rev. D **60**, 054503 (1999).
- [18] MILC Collaboration, K. Orginos and D. Toussaint, Phys. Rev. D **59**, 014501 (1999).
- [19] F. Karsch, E. Laermann, and A. Peikert, Phys. Lett. B **478**, 447 (2000).
- [20] G. P. Lepage, Phys. Rev. D **59**, 074502 (1999).
- [21] M. Hasenbusch, Phys. Rev. D **59**, 054505 (1999).
- [22] APE Collaboration, M. Albanese *et al.*, Phys. Lett. B **192**, 163 (1987).
- [23] H. Kluberg-Stern, A. Morel, O. Napoly, and B. Petersson, Nucl. Phys. **B220**, 447 (1983).
- [24] R. Gupta, G. Guralnik, G. W. Kilcup, and S. R. Sharpe, Phys. Rev. D **43**, 2003 (1991).
- [25] R. Sommer, Nucl. Phys. **B411**, 839 (1994).
- [26] ALPHA Collaboration, M. Guagnelli, R. Sommer, and H. Wittig, Nucl. Phys. **B535**, 389 (1998).
- [27] F. Niedermayer, Nucl. Phys. B (Proc. Suppl.) **53**, 56 (1997).
- [28] R. Gupta *et al.*, Phys. Rev. Lett. **61**, 1996 (1988).
- [29] J. Apostolakis, C. F. Baillie, and G. C. Fox, Phys. Rev. D **43**, 2687 (1991).
- [30] M. Hasenbusch and S. Meyer, Phys. Rev. D **45**, 4376 (1992).
- [31] U. Wolff, Phys. Lett. B **284**, 94 (1992).
- [32] M. Creutz, Phys. Rev. D **36**, 515 (1987).
- [33] F. R. Brown and T. J. Woch, Phys. Rev. Lett. **58**, 2394 (1987).
- [34] K. M. Decker and P. de Forcrand, Nucl. Phys. B (Proc. Suppl.) **17**, 567 (1990).
- [35] R. Gupta, G. W. Kilcup, A. Patel, S. R. Sharpe, and P. de Forcrand, Mod. Phys. Lett. A **3**, 1367 (1988).
- [36] UKQCD Collaboration, S. P. Booth *et al.*, Phys. Lett. B **275**, 424 (1992).
- [37] U. Wolff, Phys. Lett. B **288**, 166 (1992).
- [38] M. Grady, Phys. Rev. D **32**, 1496 (1985).
- [39] M. Creutz, in Algorithms for Simulating Fermions, Advanced Series on Directions in High Energy Physics- Vol. 11, edited by M. Creutz.
- [40] A. Hasenfratz and T. A. DeGrand, Phys. Rev. D **49**, 466 (1994).
- [41] A. Duncan, E. Eichten, and H. Thacker, Phys. Rev. D **59**, 014505 (1999).
- [42] A. Duncan, E. Eichten, R. Roskies, and H. Thacker, Phys. Rev. D **60**, 054505 (1999).
- [43] P. de Forcrand, Nucl. Phys. B (Proc. Suppl.) **73**, 822 (1999).
- [44] O. Martin and S. W. Otto, Phys. Rev. D **31**, 435 (1985).
- [45] A. Hasenfratz and F. Knechtli (in preparation).
- [46] S. Gottlieb, W. Liu, D. Toussaint, R. L. Renken, and R. L. Sugar, Phys. Rev. D **35**, 2531 (1987).
- [47] S. Duane, A. D. Kennedy, B. J. Pendleton, and D. Roweth, Phys. Lett. B **195**, 216 (1987).
- [48] T. DeGrand, A. Hasenfratz, and F. Knechtli (in preparation).
- [49] T. Takaishi and P. de Forcrand, Nucl. Phys. B (Proc. Suppl.) **94**, 818 (2001).
- [50] I. Montvay, Nucl. Phys. **B466**, 259 (1996).